Publications of the Astronomical Society of the Pacific
108: 1135–1138, 1996 December

Measuring the Atmospheric Influence on Differential Astrometry: A Simple Method Applied to Wide-Field CCD Frames

N. ZACHARIAS[1]

U.S. Naval Observatory, 3450 Massachusetts Avenue, N.W., Washington, DC 20392
Electronic mail: nz@pyxis.usno.navy.mil

Received 1996 May 14; accepted 1996 August 28

ABSTRACT. Sets of short-exposure, guided CCD frames are used to measure the noise added by the atmosphere to differential astrometric observations. Large nightly variations that are correlated with the seeing have been found in the data obtained over two years at the KPNO and CTIO 0.9-m telescopes. The rms noise added by the atmosphere, after a linear transformation of the raw x,y data, is found to be 3–7 mas, normalized to 100-s exposure time and a field of view of 20 arcmin near the zenith. An additional nearly constant noise (base level) of 8.5 mas = 0.012 pixel is found for the KPNO and 6.0 mas = 0.015 pixel for the CTIO telescope. This implies that a ground based, all sky, astrometric survey from guided CCD frames is more likely limited by the base-level noise than by the atmosphere and could reach an accuracy better than 10 mas under good seeing conditions.

1. INTRODUCTION

Turbulence in the Earth's atmosphere adds noise to ground-based astrometric observations. Semiempirical and empirical results have been published previously (e.g., Lindegren 1980; Kleine 1983; Han 1989; Monet and Monet 1992, Han and Gatewood 1995). This effect ultimately limits the accuracy of ground-based astrometric observations, and it is important to find these limits. The effect is largest, about 100 mas, for absolute astrometry. For differential astrometry, previous investigations have dealt with *angular separation* measures. The effect is found to be at the 1–2 mas level for arcminute separations and several minutes integration time (Han and Gatewood 1995), e.g., applicable to double star and parallax observations.

Here we will go one step further and define $\sigma_{\rm atm}$ as the added noise introduced by the atmosphere to astrometric observations, after an orthogonal or linear mapping model has been applied to the x,y data of guided exposures. This is more appropriate for astrometric imaging observations, because such a mapping model is used for the calibration of the x,y data to the reference star positions anyway, thus absorbing terms like scale factor and field rotation. The proposed technique in principle can be used with photographic plates as well as with CCD imaging, although the use of CCDs is more likely to show any atmospheric effect due to usually shorter exposure times and higher internal precision.

The dependence of $\sigma_{\rm atm}$ on integration time is well known to be $\sigma_{\rm atm} \sim t^{-1/2}$ and we assume this relationship here in our definition of $\sigma_{\rm atm}$. The dependence of $\sigma_{\rm atm}$ on the field of view (FOV) is approximately known to be $\sigma_{\rm atm} \sim (\mathrm{FOV})^{-1/3}$ (e.g., Han 1989), at least for fields smaller than about half a degree, and will not be investigated here. Our goal is to determine the range of $\sigma_{\rm atm}$ for different nights and atmospheric conditions and look for a dependence on seeing, as determined from the full width at half maximum (FWHM) of the image profiles.

2. METHOD

A simple method is introduced here to measure $\sigma_{\rm atm}$ based on direct CCD imaging without the need for further instrumentation. CCD frames have been taken of fields with a high star density and reduced by standard procedures including bias removal and flat fielding. Circular symmetric two-dimensional Gaussian image profiles have been fitted by least-squares methods to the flat-fielded CCD pixel data. Figure 1 gives an example for the standard error in position plotted versus instrumental magnitude for individual images. Stars within a dynamic range from the saturation limit (here set to tenth magnitude) to about five magnitudes fainter, display an almost constant level of precision for the x,y position as obtained by the image profile fit. The positional error increases for fainter stars because of the smaller S/N ratio and for brighter stars because of the model insufficiencies (saturated pixels, diffraction spikes). Images well above the average position error for their magnitudes are either from double stars or galaxies and have been excluded from this investigation. This diagram does not change with exposure time, except for a shift along the magnitude scale and the number of images available in a given range of instrumental magnitudes.

Assume two CCD frames of equal exposure times have been taken within a short period of time under the same conditions (atmosphere and telescope). The field center of the second exposure has been shifted by a few pixels with respect to the first one. Thus, independent observations have been obtained with images of the same star located on dif-

[1]With Universities Space Research Association (USRA), Division of Astronomy and Space Physics, Washington, DC, based on observations made at KPNO and CTIO.

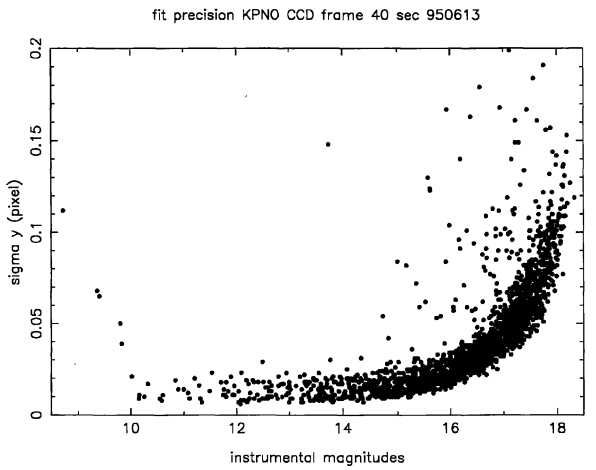

FIG. 1—Precision in the y coordinate (along α) for star image profile fits of a typical CCD frame vs. instrumental magnitude. This example is from a 40-s exposure obtained at the KPNO 0.9-m telescope in 1.″6 seeing. The scale is 0.01 pixel = 6.8 mas.

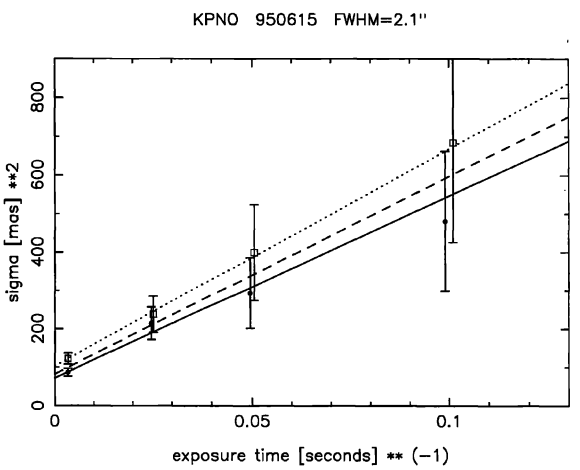

FIG. 2—Variance of x,y transformation ($\sigma^2=\sigma^2_{\rm trans}/2$) in mas^2 vs. inverse exposure time in s^{-1} for an example from KPNO observations. The filled circles are for the x coordinate (δ) and the open boxes are for the y coordinate (α). Fit results are shown as dotted, full, and dashed lines (y only, x only, both coordinates).

ferent pixels of the CCD for both frames. Only the repeatability of the observations is investigated here, so no attempt has been made to convert the x,y measures into right ascensions and declinations. All error contributions related to field distortions are avoided because the same approximate field center has been used for both exposures.

The x,y coordinates of the first frame are transformed into the system of the x,y coordinates of the second frame with a least-squares fit using either a linear or orthogonal model. Only those stars within the magnitude range of almost constant fit precision, as described above, have been used for this transformation. The variance of the transformation between the two exposures, $\sigma^2_{\rm trans}$, is

$$\sigma^2_{\rm trans}=2(\sigma^2_{\rm atm}+\sigma^2_b),$$

with $\sigma_{\rm atm}$ being the contribution from the atmosphere and σ_b the remaining error contribution—the base level—as inherent in our procedure and instrument (model insufficiencies, digitization errors, etc.), for each individual CCD frame. Defining σ_a from $\sigma_{\rm atm}=\sigma_a t^{-1/2}$ with exposure time t in seconds, we arrive at

$$\sigma^2_{\rm trans}/2=\sigma^2_a t^{-1}+\sigma^2_b=\sigma^2,$$

which is a linear relationship between the observable quantity σ^2 and the nearly error-free parameter t^{-1}. Assuming constant observational conditions for the time to take more sets of CCD frame pairs for other exposure times, we can solve for σ_a and σ_b.

3. OBSERVATIONS

Observing runs for the Radio-Optical Reference Frame (RORF) Project (Johnston et al. 1991) have been conducted from 1994 to 1996 at the 0.9-m telescopes on Kitt Peak and Cerro Tololo (Zacharias et al. 1995). The KPNO 0.9-m telescope has a scale of 0.″68/pixel and a FOV of 23.′2, while those numbers are 0.″40/pixel and 13.′6 for the CTIO telescope.

A few CCD frames were specifically taken to investigate the limits set by the atmosphere on astrometric accuracy. Fields with a high star density (close to the Milky Way) and close to the zenith, if possible, were observed close to the meridian. For most of the selected fields, two frames of 40-, 20-, and 10-s exposure time each were taken with the same Gunn r filter in addition to the long exposures for the RORF project. An off-axis autoguider was used with guide stars selected close to the edge of the main FOV. The integration and correction cycle time was set to about 1 s and the system was guiding for at least 10 s before the start of a new exposure.

Figure 2 shows an example of σ^2 plotted versus t^{-1} for the four exposure times. A linear model has been used for the x,y transformations. The filled circles and open squares are the results for the x and y coordinates, respectively (along δ, α for the KPNO telescope).

Because there are more faint than bright stars, the longer exposure frames show more stars near the saturation limit than the short exposure frames. Also, for a given constant number of stars used for different transformations, the value of $\sigma_{\rm trans}$ is better determined for longer exposure times because of the smaller scatter in the x,y transformation data due to better image definition from the longer integration time. Thus, weights have been assigned to each measured $\sigma^2_{\rm trans}$ value. Let $E(y)$ be an estimate of the standard error of the quantity y and $y=x^2$ with $x=\sigma_{\rm trans}$; then we have from the error propagation law

$$E(y)=E(x^2)=2xE(x).$$

$E(x)$ is here the standard error of the mean, using all $n_{\rm stars}$ star pairs for the transformation, thus

$$E(x)=\sigma_{\rm trans}/\sqrt{n_{\rm stars}}.$$

Putting everything together, we arrive at the adopted formula

TABLE 1
Observations and Results

Tel.	Date (ymd)	z degree	FWHM (arcsec)	nexp	σ_a (mas $s^{-1/2}$)	error (mas $s^{-1/2}$)	σ_b (mas)	error (mas)	σ_{an} (mas)
K	940420	6	2.00	4	62	9	7.0	0.5	5.9
					74	6	7.5	0.3	7.1
K	940422	21	2.10	4	39	15	10.2	1.0	3.6
					50	16	10.3	1.2	4.5
K	940423	17	2.65	3	68	13	8.2	3.0	6.3
					60	15	10.1	2.9	5.5
K	941020	44	1.70	4	43	12	9.1	0.9	3.1
					35	20	12.0	1.2	2.5
K	950613	1	1.65	4	31	7	8.8	0.5	3.0
					36	10	9.0	0.7	3.5
K	950615	12	2.10	4	72	6	9.1	0.5	6.8
					80	7	8.9	0.6	7.5
K	950617	15	1.30	4	38	6	7.9	0.5	3.6
					39	7	8.0	0.6	3.7
K	960105	15	1.20	5	39	8	8.8	0.9	3.6
					45	7	9.2	0.9	4.1
C	941215	17	1.35	5	54	7	5.8	0.7	6.0
					65	10	7.4	1.1	7.3
C	950213	1	1.30	4	39	6	6.5	0.6	4.4
					75	4	9.2	0.5	8.5
C	950917	1	1.60	4	67	6	5.9	0.8	7.6
					72	15	7.8	1.6	8.2

error estimate on $\sigma^2_{\text{trans}} = 2\sigma_{\text{trans}} \dfrac{\sigma_{\text{trans}}}{\sqrt{n_{\text{stars}}}}$.

The weighting is not critical for the determination of the slope itself, i.e., for the atmospheric contribution. The determination of the base level and the error estimates on the results depend more strongly on the choice of the weighting algorithm. This conclusion was obtained from tests made with different weighting algorithms, including unweighted reductions.

A weighted least-squares fit was performed with the σ^2 vs. t^{-1} data points, in order to obtain the slope and constant of the straight line predicted by the theory. Fit results for each axis separately (dotted, full line) as well as for the combined data (dashed line), are shown in Fig. 2.

4. RESULTS

From the straight-line fit of the σ^2 vs. t^{-1} plots for the combined data of both axes, σ_a and σ_b, and their errors were calculated. Table 1 lists all observations and results. The first line for each observation shows the result from the linear transformation model, while the second line shows the result as obtained with the orthogonal model. The last column displays σ_{an}, which is σ_a normalized to 100-s exposure time and a FOV of 20 arcmin for the zenith, obtained from

$$\sigma_{an} = \sigma_a \left(\frac{1^s}{100^s}\right)^{1/2} \left(\frac{20'}{\text{FOV}}\right)^{1/3} \cos z,$$

with FOV being the field of view in arcmin as used for the x,y transformations and z being the mean zenith distance while observing the field. Figure 3 shows results for σ_{an} obtained with the linear x,y transformation model plotted versus FWHM, scaled to the zenith with a $\cos z$ factor, adopted from Lindegren (1980).

5. DISCUSSION

There is a large nightly variation in the atmospheric influence on the observed star positions, which is correlated with seeing (FWHM), but "the seeing value" alone does not determine σ_{an}. On the average we obtain $\sigma_{an} \approx 3$ mas and 6 mas for 1 and 2 arcsec seeing, respectively.

The results obtained with the orthogonal x,y transformation model give on the average larger numbers for σ_{an} by about 10%. This is expected, because fewer parameters will model less of the real atmospheric effects.

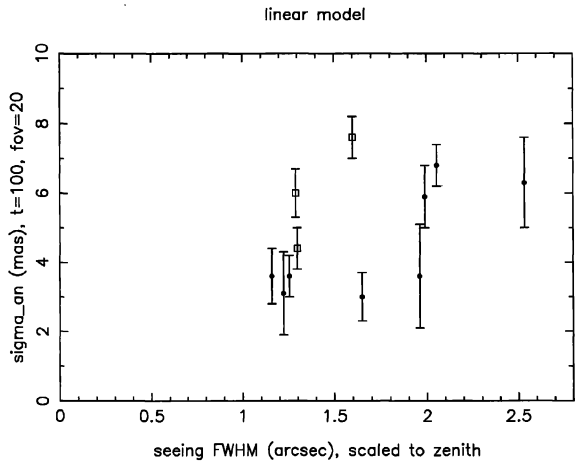

FIG. 3—Error contribution by the atmosphere to differential astrometry vs. FWHM of image profiles, scaled to the zenith. Full circles and open boxes show results from the KPNO and CTIO telescopes, respectively. Only results of the linear x,y transformation model are shown here.

All our results hold only for this type of guided imaging observing procedure. For differential transit circle or scanning mode observations, the modeling of the atmospheric effects is different, as will be the residual effects caused by the atmosphere on the astrometric results (Stone et al. 1996).

Lindegren (1980) obtained standard errors for observing the separation of stars, i.e., a different kind of differential astrometry from that investigated here. His result, scaled to 100-s exposure time and a mean separation of 10′ (comparable to our 20′ FOV), is about 19 mas. Results by Han (1989) would lead to 14 mas for this case. Both Lindegren's and Han's results are obtained in medium seeing conditions ($\approx 2''$); thus they have to be compared to our 6 mas, which is a factor of 2–3 smaller. Scaled to a 100-s exposure time and a star separation of 10′, Han and Gatewood (1995) found σ_{an} = 5.4 mas from star trail observations obtained from Mauna Kea. Our result is 3 mas for good seeing, which is smaller by almost a factor of 2.

Separation measurements made at the 61-in. Flagstaff telescope result in an atmospheric contribution of 9–28 mas for this case, depending on the night (Monet and Monet 1992; Monet 1996). Again our result is a factor of 2–3 smaller. Similar to our results, Monet and Monet find a lose correlation with seeing, which ranged from FWHM=1.″2 to 2.″3. According to a hypothesis (Monet 1996), local effects near the dome cause some of the "astrometric seeing," not correlated with the general FWHM.

This difference between our results and those obtained by other investigations can be explained by the different types of observations. The *simultaneous* observation of all stars in the FOV seems to be important. Moreover, our guided exposures follow correlated image motions of a star field, caused by the atmosphere, and thus reduce the noise contribution compared to other differential observing procedures. Also, a linear reduction model will give smaller residuals as compared to angular separation measurements with fewer free parameters.

As a byproduct of this method, the base level of accuracy has been determined as well. The mean of all σ_b with a standard error smaller than 1.0 mas is found to be 8.5 mas = 0.012 pixel for all KPNO observations. The corresponding result for the CTIO instrument is 6.0 mas = 0.015 pixel. These numbers are for a single observation per coordinate. The slightly smaller value for σ_b (in pixel units) for the KPNO instrument can be explained by the better optical quality of that telescope, which includes a field-flattener corrector lens. Imperfections in the CCD, the optics of the telescope, and model deficiencies contribute to this base level of astrometric accuracy, which is under further investigation (Zacharias and Rafferty 1995; Winter 1997; Zacharias 1997).

6. CONCLUSIONS

A large nightly variation (factor of 2) of the noise added by the atmosphere to differential astrometry has been found. This added noise is correlated with the seeing. In good seeing conditions ($\approx 1''$) the contribution of the atmosphere to differential astrometry can be as small as 3 mas for guided 100-s exposures and a FOV of 20 arcmin for 0.9-m aperture telescopes.

Guided exposures with simultaneous observation of all stars in the FOV give a considerable (about a factor of 2) advantage over angular separation measurements made with other differential astrometric observing techniques.

For a 1 degree FOV astrometric survey telescope, our result scales to 4.3 mas noise contributed by the atmosphere for 100-s exposures. This is considerably less than previously expected. Thus the limit to ground-based wide-field astrometric observations as set by the atmosphere has not yet been reached for long integration times ($\geq$100 s) because of the relatively large base-level noise of $\approx$0.015 pixels, which is on the order of 6–15 mas, depending on the sampling.

I would like to thank Kitt Peak and Cerro Tololo Observatories for granting observing time. I am grateful to M. I. Zacharias for assistance in observing and reduction of the CCD frames.

REFERENCES

Han, I. 1989, AJ, 97, 607
Han, I., and Gatewood, G. D. 1995, PASP, 107, 399
Johnston, K. J., et al. 1991, in Reference Systems, Proceedings of IAU Colloq. 127, ed. J. A. Hughes, C. A. Smith, and G. H. Kaplan (Washington, DC, US Naval Observatory), p. 123
Kleine, T. 1983, dissertation, University of Hamburg
Lindegren, L. 1980, A&A, 89, 41
Monet, D. G., and Monet, A. K. B. 1992, BAAS, 24, 1238
Monet, D. G. 1996, private communication
Stone, R. C., Monet, D. G., Monet, A. K. B., Walker, R. L., Ables, H. D., Bird, A. R., and Harris, F. H. 1996, AJ, 111, 1721
Winter, L. 1997, dissertation, University of Hamburg (in preparation)
Zacharias, N., de Vegt, C., Winter, L., and Johnston, K. 1995, AJ, 110, 3093
Zacharias, N., and Rafferty, T. 1995, BAAS, 27, 1302
Zacharias, N. 1997, AJ (in preparation)